HHS Public Access
Author manuscript
Inflamm Bowel Dis. Author manuscript; available in PMC 2017 February 01.

Published in final edited form as:
Inflamm Bowel Dis. 2016 February ; 22(2): 279–292. doi:10.1097/MIB.0000000000000618.

The novel PPARγ modulator GED-0507-34 Levo ameliorates inflammation-driven intestinal fibrosis

Speca Silvia, PhD[1,2,3], **Rousseaux Christel, PhD**[4], **Dubuquoy Caroline**[4], **Rieder Florian, MD**[5], **Vetuschi Antonella, MD**[3], **Sferra Roberta, PhD**[3], **Giusti Ilaria, PhD**[3], **Bertin Benjamin, PhD**[1,6], **Dubuquoy Laurent, PhD**[1,6], **Gaudio Eugenio, MD, PhD**[7], **Desreumaux Pierre, MD, PhD**[1,2,6], and **Latella Giovanni, MD**[3]

[1]Inserm, LIRIC UMR995, F-59000 Lille, France

[2]CHRU de Lille, Service des Maladies de l'Appareil Digestif et de la Nutrition, Hôpital Claude Huriez, LIRIC – UMR995, F-59000 Lille, France

[3]Department of Life, Health and Environmental Sciences, Gastroenterology Unit, University of L'Aquila, L'Aquila, Italy

[4]IBD Lille, France

[5]Department of Pathobiology, Lerner Research Institute; Department of Gastroenterology, Hepatology & Nutrition, Digestive Disease Institute; Cleveland Clinic Foundation, Cleveland, Ohio, USA

[6]Université Lille Nord de France, Lille, France

[7]Department of Human Anatomy, University of Roma “La Sapienza”, Roma, Italy

Abstract

Background—Intestinal fibrosis is mainly associated with Crohn's disease (CD) and is defined as a progressive and excessive deposition of extracellular matrix (ECM) components. No specific anti-fibrotic therapies are available. In this study we evaluate the anti-fibrotic effect of GED, a novel PPARγ modulator[1-4].

Methods—Colonic fibrosis was induced in 110 C57BL/6 mice by three cycles of 2.5% (w/v) DSS administration for 6 weeks. The preventive effects of oral daily GED (30mg/kg/d) administration were evaluated using a macroscopic and histologic score as well as through biologic endpoints. Expression of main markers of myofibroblasts activation was determined in TGF-β-stimulated intestinal fibroblasts and epithelial cells (IECs).

Results—GED improved macroscopic and microscopic intestinal lesions in dextran sulfate sodium (DSS) treated animals and reduced the profibrotic gene expression of Acta2, COL1a1 and Fn1 by 1.48 folds ($p< 0.05$), 1.93 folds ($p< 0.005$) and 1.03 fold ($p< 0.05$), respectively. It reduced protein levels of main markers of fibrosis (α-SMA and Collagen I-II), as well as the main TGFβ/

Corresponding author: Giovanni Latella, MD, Gastroenterology Unit, Department of Life, Health and Environmental Sciences, University of L'Aquila, Piazza S. Tommasi, 1- Coppito, 67100 L'Aquila, Italy., giolatel@tin.it, Telephone: +39-0862-434735, Mobile: +39-3387361784, Fax: +39-0862-433425.

Conflict of interest: For remaining authors none were declared.

Smad pathway components. GED also decreased the IL-13 and CTGF expression by 1.89 folds ($p<0.05$) and 2.2 folds ($p<0.005$), respectively. GED inhibited TGF-β-induced activation of both fibroblast and IEC cell lines, by regulating mRNA expression of αSMA and fibronectin and restoring the TGF-β-induced loss of IEC markers. GED treatment also reduced the TGFB and ACTA1 expression in primary human intestinal fibroblasts from ulcerative colitis (UC) patients.

Conclusions—GED ameliorates intestinal fibrosis in DSS-induced chronic colitis in mice and regulates major pro-fibrotic cellular and molecular mechanisms.

Keywords

Inflammatory bowel disease; intestinal fibrosis; TGF-β signal transduction pathway; new anti-fibrotic therapeutic strategies; peroxisome-proliferator activated receptor

Introduction

Intestinal fibrosis is a common complication of inflammatory bowel disease (IBD) occurring both in ulcerative colitis (UC) and Crohn's disease (CD), but its prevalence and severity is significantly higher in CD with intestinal strictures occurring in approximately at least one-third of patients[1-4].

The permanent scarring and the consequent luminal narrowing and obstruction, as well as structural changes and colonic motility disorders, represent the evident display of an intestinal fibrotic process in which the undisputed feature is the excessive accumulation of extracellular matrix (ECM) components[1-5]. The ECM deposition is classically attributed to the activation of myofibroblasts, alpha smooth muscle actin (α-SMA) positive cells, with high potential for proliferation, migration and contraction. Myofibroblasts progenitors include resident mesenchymal cells (fibroblasts, sub-epithelial myofibroblasts and smooth muscle cells), stellate cells, pericytes, and intestinal or bone marrow derived stem cells, as well as epithelial and endothelial cells by a process known as epithelial/endothelial-mesenchymal transition[6, 7]. The myofibroblasts activation is controlled by several pro-fibrotic mediators, orchestrated by the transforming growth factor (TGF)-β/small mother against decapentaplegic (Smad) pathway[8-13]. Overexpression of the main components of this pathway is, indeed, found in fibrostenotic CD, as well as in animal models of experimental intestinal fibrosis [14, 15]. In addition, the disruption of the TGF-β/Smad signaling pathway, either by the loss of Smad3, or the increase of its negative regulator Smad7, seems to confer resistance to the experimental colorectal fibrosis in rodents [7, 16, 17].

An enticing candidate able to counteract the profibrogenic effect of TGF-β1 is the peroxisome-proliferator activated receptor (PPAR)γ[18, 19], a member of ligand-activated transcription factors of nuclear hormone receptor superfamily, with pleiotropic effects on lipid metabolism, inflammation, and cell proliferation. A significantly impaired PPARγ expression was observed in colonic epithelial cells of UC patients, suggesting that the disruption of PPARγ signaling may represent a critical step of the IBD pathogenesis[20]. Anti-inflammatory action of 5-Aminosalicylic acid (5-ASA), the most common treatment of

IBD, is mainly due to the activation of PPARγ[21], however 5-ASA not seem to have anti-fibrotic effects in IBD [22].

Although the role of PPAR-γ as innate protector against excessive fibrogenesis is well established[23], treatments able to prevent or improves intestinal fibrosis are not currently known [13, 23-25].

In this study, we evaluate the potential anti-fibrotic action of a new PPARγ modulator, GED-0507-34 Levo (GED), in intestinal fibrosis. This ligand is an enantiomer belonging to the aminophenyl-methoxy-propionic acid family, with strong affinity for PPARγ and strong intestinal anti-inflammatory properties (100-150 fold greater than 5-ASA), mainly related to its ability to inhibit the NF-κB transactivation[26, 27].

Materials and Methods

Animals

A total of 110 wild type C57BL/6 mice, purchased from Janvier (Le Genest-St-Isle, France) were included in the study. All mice were maintained in a specific pathogen-free facility, fed with a standard diet and given free access to water under constant room temperature with a 12h light/12h dark cycles. Animal experiments were performed according to the governmental guidelines N° 68/609/CEE.

Induction of chronic colitis—Chronic colitis and fibrosis were induced in mice by oral administration of 2.5% (w/v) DSS (MW: 36,000–44,000, purchased from TdB Consultancy, Uppsala, Sweden) dissolved in tap water and administrated *ad libitum* for three cycles (5 day DSS followed by 7 days of tap water). Control groups received tap water only. Animals were monitored daily for food and fluid intake and were weighed at the beginning of the study and thereafter regularly every three days.

Drugs—GED-0507-34 Levo, purchased from Nogra Pharma Ldt was dissolved in a solution containing 0.5% Carboxymethylcellulose sodium salt (Sigma-Aldrich) and 1% Tween 80 and administrated at the dose of 30mg/Kg/day by oral gavage (100μl/mouse). 150 mg/kg 5-ASA (Pentasa, Ferring Pharmaceuticals) was mixed with standard chows and daily administrated. GW9662 (GW) (Sigma-Aldrich), a selective PPARγ inhibitor, was also administrated by intraperitoneal injection at the dose of 1 mg/kg/day combined with GED treatment. All drugs was administrated at the beginning of second cycle of DSS (day 12).

Experimental design—Two independent experiments have been performed. In the first one the mice were randomly divided into three groups: i. control group receiving only tap water (H_2O group, n=10); ii. DSS-treated mice (DSS group, n=25); iii. DSS-treated mice receiving 30 mg/kg/day GED (DSS+GED group, n=25).

In the second experiments 5 groups (n=10 mice per group) have been compared: i. control group (CTRL group); ii. DSS-treated mice (DSS group); iii. DSS-treated mice receiving 30 mg/kg/day GED (DSS+GED group); iv. DSS-treated mice receiving 150 mg/kg/day 5-ASA

(DSS + 5-ASA group); v. DSS-treated mice receiving both 30 mg/kg/day GED and 1 mg/Kg/day GW (DSS + GED + GW group).

Clinical evaluation and sample recovery—Animals were observed daily for fluid intake, weight changes, and examined for signs of colitis including weight loss, diarrhea (scored on a 0–2 scale, as follows: 0 = absence, 1 = mild, 2 = severe) and rectal bleeding, assessed with the ColoScreen III Lab Pack (Elitech, Salon-de-Provence, France) and prolapse, (scored as 0= absence, 1=presence) [17].

Four days after the last DSS cycle administration, the animals of each group were euthanized by cervical dislocation under deep CO_2 anaesthesia and underwent laparotomy. The colons were visualized and rapidly excised. The colonic tissue samples were, immediately, fixed in 4% buffered formaldehyde for histological and immunohistochemical assays, or frozen for further molecular investigations.

Assessment of macroscopic and microscopic colonic lesions—The colonic length and weight were measured and then scored for macroscopic lesions. The macroscopic colonic lesions were scored by three independent observers (S.S., R.C. and D.C.) who were unaware of the treatment. They assessed and scored the individual macroscopic colonic lesions on a 0–2 scale, as follows: colonic adhesions (0 = absence, 1 = mild/focal-zonal, 2 = severe/diffuse); colonic dilation (0 = absence, 1 = mild, 2 = severe); colonic thickness (0 = normal, 1 = mild increase, 2 = marked increase, > 3 mm)[17].

The sum of the scores of colonic lesions was expressed as total macroscopic score[17]. Interobserver agreement was 95% for all appointed score.

Colonic specimens of all animals were washed and immediately fixed in 10% buffered formalin in phosphate buffer saline (PBS) at pH 7.4 for 3 h at room temperature followed by the standard procedure for paraffin embedding. Serial 3-μm sections were stained with haematoxylin and eosin (H&E) to assess the degree of inflammation and with Masson's trichrome to detect connective tissue and fibrosis. The stained sections were then observed under an Olympus BX51 Light Microscope (Olympus, Optical Co. Ltd, Tokyo, Japan). Two pathologists (A.V. and R.S.) independently examined and scored all histological sections of the colonic samples in double-blind, according to the presence of ulcerations (0=absent, 1= small ulcers, 2= big ulcers), degree of inflammation (0=absent, 1= mild, 2= moderate and 3=severe), depth of the lesions (0=absent, 1= lesions extending in the submucosa, 2= lesions in the muscolaris propria and 3= lesions in the serosa) and degree of fibrosis (0=absent; 1= mild, 2=moderate and 3=severe). The sum of these scores was expressed as total microscopic score as previously reported[17]. The degree of intestinal inflammation was scored as absent, mild, moderate or severe, according to the density and extent both of the acute and chronic inflammatory infiltrate, loss of goblet cells, and bowel wall thickening. Intestinal fibrosis was scored as mild, moderate or severe, depending on the density and extent of trichrome-positive connective tissue staining and disruption of tissue architecture, as previously described [17].

Immunohistochemistry—Fixed tissue specimens from the colon were dehydrated in a graded ethanol series, and embedded in low-temperature-fusion paraffin. Serial 3-μm-thick sections were incubated for 40 min. in methanol and 3% hydrogen peroxide solution and then rinsed in PBS.

Thereafter, sections were incubated overnight at 4°C with specific antibodies (Santa Cruz Biotechnology Inc., Santa Cruz, CA, USA) to α-SMA (SC-32251), collagen types I-III (SC-8784; SC-8781), TGF-β1 (SC-146), connective tissue growth factor (CTGF) (SC-14939), pSmad3 and Smad3 (SC-6202), and IL-13 (A130D 12G5 1E4; Antibodies-online), according to the manufacturer's protocols. The samples were washed for 5 min with PBS and incubated with streptavidin-biotin-peroxidase conjugated kit (Dako LSAB Corporation, cod K0675, Dako-Cytomation, Milano). After rinsing in PBS for 10 min the sections were incubated with 3,3-Diaminobenzidine (DAB, Sigma Aldrich) for 1-3 min. The specificity of the immune reaction was ensured by omitting the primary antibodies. Finally the samples were counterstained with Mayer's Haematoxylin and observed under a photomicroscope (Olympus BX51 Light Microscope; Olympus, Optical Co. Ltd., Tokyo, Japan). Quantitative comparison of immunohistochemical staining was achieved by digital image analysis and expressed as percentage of expression in the total software-classified areas using the ImageJ public domain software (W. S., Rasband, ImageJ, U. S. National Institutes of Health, Bethesda, MD; http://rsb.info.nih.gov/ij/, 1997–2011)

Western blot analysis—Approximately 0.5 cm of frozen colonic samples were cut and mechanically homogenized in RIPA Buffer containing 50 mM Tris HCl pH 7.6, 150 mM Sodium Chloride (NaCl; MW: 58,44; Sigma Aldrich) 1.5 mM Magnesium Chloride ($MgCl_2$; MW: 95.21 g/mol; Sigma Aldrich) 5mM Ethylenediaminetetraacetic acid (EDTA; MW: 292.24 g/mol) 1% Triton-X and 10% Glycerol, supplemented with 100 mM Sodium Fluoride (NaF: MW: 41.99 g/mol; Sigma Aldrich), 2 mM Sodium Orthovanadate (Na_3VO_4; MW: 183.91 g/mol; Sigma Aldrich), 10 mM Sodium Pyrophosphate (NaPPi; MW: 446.06 g/mol; Sigma Aldrich), 1 mM Phenylmethanesulfonyl fluoride (PMSF; MW: 174.19 g/mol; Sigma Aldrich) and an appropriate protease-inhibitor cocktail (cOmplete, Mini, EDTA-free; Roche).

30 μg of protein for each sample were separated by Sodium dodecyl sulfate polyacrylamide gel electrophoresis (SDS-PAGE) and transferred. into a 100% pure nitrocellulose membranes that were incubated (according with a specific protocol for each antibody) with primary antibodies directed against Collagen-I, CTGF, GAPDH (purchased from Abcam, Cambridge, UK; 1:1000 for 2 h at room temperature), and IL-13 (purchased from Antibodies-online; 1:1000 for 2h at room temperature) diluted in 5% not fat-milk in Tris Buffered Saline (TBS) solution consisting of 500mM Tris, 2.8M NaCl, supplemented by 0.1% Tween-20 (TBS-T) to pH 7.4. Membranes were subsequently washed in TBS-T 0.1% and incubated with secondary horseradish peroxidase-conjugated antibodies (anti-Rabbit and anti-Mouse; Sigma Aldrich; 1:20000 for 1 h at room temperature) diluted in 5% not fat-milk in 0.1% TBS-T. Finally, immunodetection was performed with SuperSignal West Pico chemiluminescent substrate (Thermo Scientific Pierce, Erembodegem) according to manufacturer's protocol. Membranes were exposed to autoradiography film (Fuji Photo Film Co., Dusseldorf, Germany). Optical density of target bands was determined using a

computer-assisted densitometer and the ImageJ public domain software (W. S., Rasband, ImageJ, U. S. National Institutes of Health, Bethesda, MD; http://rsb.info.nih.gov/ij/, 1997–2011). Tissue levels were expressed as units of Optical Density (OD) per quantity of total proteins, normalizing with internal control glyceraldehyde-3-phosphate dehydrogenase (GAPDH) and the results were expressed as percentage of control groups.

Quantitative RT-PCR—Approximately 0.5 cm of frozen colonic samples were cut and mechanically homogenized. Thus, total RNA was extracted with a Nucleospin RNA kit (Macherey-Nagel, Hoerdt, France). After RNAse inactivation, the total RNA was cleaned of traces genomic DNA via a DNAse treatment and eluted in RNAse-free, DEPC-free water. The purity of the RNA was evaluated by UV spectroscopy on a Nanodrop system from 220 to 350 nm. 1 μg of total RNA was used to perform a Quantitative RT-PCR by using LightCycler FastStart DNA Master SYBR Green I from Roche Diagnostics (Indianapolis, IN) according to the manufacturer's protocol[28]. Primers sets includes Acta2 for αSMA, Fn1 for Fibronectin, COL1a1 for Collagen I-1III, TGFB for TGF-β1, KRT20 for Cytokeratin 20 and GPA33 for Glycoprotein A33. Sequences and relative NCBI references for each gene are listed in Tab 1.

Cells

Human intestinal epithelial and fibroblast cell lines—Human intestinal epithelial cell line HT-29 (ATCC HTB-38) and human intestinal fibroblast cell line CCD-18Co (ATCC CRL-1459) were grown in Dulbecco's modified Eagle's medium (DMEM) and Eagle's Minimum Essential Medium (MEM), respectively, both supplemented with 100 U/ml penicillin, 100 μg/ml streptomycin and 10% fetal bovine serum (FBS). Cell cultures were maintained in a humidified atmosphere of 95% air and 5% CO_2 at 37°C.

Primary human intestinal fibroblasts—Primary human intestinal fibroblasts (HIF) were kindly provided by Florian Rieder from the Cleveland Clinic Foundation (Cleveland, OH, USA). Isolation, culture and characterization of these HIF cultures were assessed as previously described[22]. HIF were obtained from surgical specimens taken from healthy areas of the mucosa of patients with diverticulitis or colon cancer (considered as normal controls: HIF-NC) and UC patients (HIF-UC). HIF cultures were grown in DMEM supplemented with 100 U/ml penicillin, 100 μg/ml streptomycin 10% FBS and 2,5% 4-(2-Hydroxyethyl)piperazine-1-ethanesulfonic acid (HEPES) and maintained in a humidified atmosphere of 95% air and 5% CO_2 at 37°C.

Experimental design—Cells were seeded in 6-wells plates for 24 h, then myofibroblasts activation was induced maintaining HT29 and CCD-18Co in a medium supplemented with 10 ng/ml (4 and 6 days) and 1 ng/mL (2 and 4 days) of TGF-β1 (MW: 25 kDa; Sigma Aldrich), respectively. The medium was replaced every two days with fresh medium supplemented with TGF-β1, with or without 1 mM GED.

A treatment with 10^{-6} M GW, was also performed in CCD-18Co stimulated by TGFβ, 1 h before GED administration. Primary human fibroblasts (HIF) were treated 24 h with 1 mM GED.

Immunofluorescence—Myofibroblast activation was identified by immunofluorescent detection of α-SMA. A monolayer of HT29 and CCD-18Co was seeded on glass coverslips and treated as previously described in the experimental design, then was fixed in 4% paraformaldehyde for 15 min, and permeabilized in 0.1% Triton X-100 for 10 min at room temperature. Following fixation, slides were blocked with 3% BSA for 30 min. Subsequently, slides were incubated overnight using a specific anti-αSMA antibody (1:400). For protein visualization, AlexaFluor 594 donkey anti-mouse antibody was used. Nuclear counterstaining was performed using a mounting medium fortified with DAPI (Invitrogen). Images were scanned at 40× magnification on a LSM 510 (Zeiss). Digital images were processed with Zeiss LSM Browser.

Quantitative RT-PCR—HT29 and CCD-18Co were stimulated with 10 ng/mL and 1 ng/mL TGFβ, respectively, for 4 days. 1 mM GED-0507-34 Levo (195.22 g/mol) was administrated during all the stimulation period with TGFβ. Thus, total RNA was extracted with a Nucleospin RNA kit (Macherey-Nagel, Hoerdt, France). After RNAse inactivation, the total RNA was cleaned of traces genomic DNA via a DNAse treatment and eluted in RNAse-free, DEPC-free water. The purity of the RNA was evaluated by UV spectroscopy on a Nanodrop system from 220 to 350 nm. 1 μg of total RNA was used to perform a Quantitative RT-PCR by using LightCycler FastStart DNA Master SYBR Green I from Roche Diagnostics (Indianapolis, IN) according to the manufacturer's protocol[28]. Primers sets included ACTA1 for αSMA, FN1 for Fibronectin, COL1A1 for Collagen I-1III, TGFB for TGF-β1, KRT20 for Cytokeratin 20 and GPA33 for Glycoprotein A33. Sequences and relative NCBI references for each gene are listed in Tab 1.

A critical threshold cycle (Ct) value, indicating the cycle number at which the DNA amplification was first detected, was determined for each reaction. Relative gene expression value was calculated as $E=2^{-\Delta Ct}$, where ΔCt is the difference in crossing points between GAPDH and each gene.

Statistical analysis—Statistical analyses were performed using Kruskal-Wallis non parametric ANOVA. Post-hoc comparisons between pairs of groups were assessed by using Wilcoxon rank sum test. Results were expressed as means ± SEM. A p-value < 0.05 was considered statistically significant.

Results

GED improves DSS-induced chronic colitis and fibrosis in mice in a PPARγ dependent manner

Macroscopic features of DSS-induced chronic colitis—At day 40 the mice were euthanized and colons were subjected to a first morphological observation. Colonic shortening and dilatation were clearly visible in the majority of DSS-treated mice and a restoration of a healthy colon features in mice receiving DSS was associated with GED administration.

A less efficacy was observed in mice treated by 5-ASA, while the GW prevented the GED ability to improve the typical colonic aspect associated to a chronic DSS administration (Fig. 1A).

The ratio weight/length of the colon was used as further indicator of inflammation and fibrosis. A significant increase of this ratio was observed in the DSS-receiving mice compared to control mice (2.1370 ± 0.054 vs 1.003 ± 0.0215) ($p < 0.005$). Oral GED administration led to a significant restoration of colon weight and length (Tab. 2). The colon weight/length ratio was, thus, reduced by 48% by GED compared to DSS-treated mice (1.648 ± 0.086 vs 2.1370 ± 0.054) ($p < 0.005$), while any significant decrease was observed in mice receiving 5-ASA. In addition, the GW administration prevented the significant reduction of the colon weight/length ratio in DSS-treated mice receiving GED (Fig. 1B).

The chronic administration of DSS was associated to a total macroscopic score equal to 3.46 ± 0.343 ($p < 0.005$) on a scale ranging from 0 to 6. A lower rate of colonic lesion was observed in DSS + GED group, determining a significantly reduction by 45% of total macroscopic score, compared to DSS-treated mice (1.87 ± 0.2675 vs 3.4 ± 0.343, $p < 0.01$, respectively) (Fig.1C).

Mice fed with 5-ASA-enriched chows, as well as mice simultaneously treated by GED and GW, did not show improvement of colonic parameters and lesions associated to the chronic DSS administration (Tab. 2), neither a decrease of the total macroscopic score compared to DSS group (Fig.1C). All macroscopic observations are summarized in Tab. 2.

Microscopic features of DSS-induced chronic colitis—Mice receiving DSS showed diffuse signs of colorectal inflammation involving *mucosal* and *submucosal* layers and characterized by increased infiltrate of inflammatory cells, decrease of goblet cells, reduction and alteration of crypt architecture and presence of erosions and ulcerations. A significant increase of collagen deposition in the *mucosa*, *submucosa* and *serosa* layers was observed in DSS-treated mice compared to control mice. Daily GED administration ameliorated histological signs of both colonic inflammation and fibrosis in DSS-treated mice, while mice subject to chronic DSS administration and fed with 5-ASA enriched chows did not show any improvement of both parameters. The GED ability to control inflammation and collagen deposition was lost when administrated together with GW (Fig. 2A).

The chronic DSS administration was associated with a total microscopic score equal to 5.74 ± 0.59 ($p < 0.005$), while GED led the significant reduction by 34% of total microscopic score compared to DSS-treated mice (3.77 ± 0.4436 vs 5.74 ± 0.5889, respectively, $p <$ 0,01), effects not observed neither in mice receiving 5-ASA-enriched chows, nor in GED treated mice simultaneously receiving GW (Fig. 2B).

GED, but not 5-ASA, specifically induces downregulation of the colonic mRNA expression of main profibrotic genes. Quantitative RT-PCR performed on frozen colonic specimens, showed as Acta2, COL1a1 and Fn1 expression was significantly induced by the chronic DSS administration by 2.97 folds ($p < 0.01$), 2.89 folds ($p < 0.01$) and 2.10 ($p < 0.05$), respectively. The significant increase of mRNA expression of all analyzed genes was

regulated by GED by 1.48 folds ($p< 0.05$), 1.93 folds ($p< 0.005$) and 1.03 fold ($p< 0.05$). In addition, 5-ASA did not significant regulate the increased expression of Acta2 and Fn1 genes in DSS-treated mice, although it was able to specifically control the COL1a1 expression. The GED effect in DSS-treated mice was, also, lost in combination with GW (Fig. 3).

GED reduced the colonic expression of main markers of fibrosis—α-SMA and Collagen I-III expression, considered as main markers of fibrosis, was assessed by immunohistochemical and immunoblotting assays. Comparison of immunohistochemical staining showed an increased expression of both α-SMA and Collagen I-III, in mice with DSS-induced chronic colitis compared to control mice (Fig. 4A).

Daily oral GED administration in mice with DSS-induced chronic colitis downregulated α-SMA and Collagen I-III expression compared to the untreated DSS group, while 5-ASA was unable to regulate the protein expression of both markers. In addition, the GW administration prevented the GED-induced decrease of α-SMA and Collagen I-III expression in DSS-treated mice.

A consistent increase of Collagen I-III by 1.88 fold in DSS-treated mice compared to controls mice was also confirmed by immunoblotting assay, a feature that was restored by GED administration (Fig. 4B).

GED downregulated the colonic expression of TGFβ, Smad3, IL-13 and CTGF —Colonic specimens were examined for IL-13, TGF-β1, SMAD2/3 and CTGF tissue expression by immunohistochemical and immunoblotting assays. As shown in Fig. 5A, DSS administration led to a consistent increase in the expression of TGF-β1 and SMAD2/3, as well as of IL-13 and CTGF compared to control mice. Daily oral GED administration was able to reduce the protein levels of these four profibrotic molecules, while 5-ASA did not induce any regulation of their tissue expression. In addition, the GW administration prevented the ability of GED to downregulate the tissue expression levels of all considered markers in DSS-treated mice (Fig. 5A).

A significant upregulation of IL-13 by 2.14 fold and of CTGF by 4.34 fold in DSS-treated mice was also confirmed by immunoblotting analysis. Daily oral administration of GED downregulated the expression of both these proteins (1.89 fold for IL-13, $p<0.05$, and 2.2 fold for CTGF, $p<0.005$) (Fig. 5B)

Human intestinal fibroblast and epithelial cell lines stimulated with TGFβ acquire a myofibroblast-like phenotype

The optimal TGF-β administration conditions inducing a differentiation of colonic intestinal fibroblast cells (CCD-18Co) to a myofibroblast phenotype were assessed by a preliminary time course study. Two days of 1 ng/mL TGF-β1 exposure significantly increased the expression of the two myofibroblast differentiation and activation markers, ACTA1 and FN1 (65% ± 4%, $p< 0.01$ and 75.5% ± 7.54%, $p<0.001$, respectively) compared to untreated cells (Fig. 6A). In addition, the marked increase of α-SMA expression was also confirmed by immunofluorescence assay: 81% of α-SMA positive cells were observed after 2 days of

TGF-β exposition, compared to not-stimulated cells; 100% of α-SMA negative cells became α-SMA positive at day 4 (Fig. 6B).

Likewise, the ability of TGF-β to induce transition of the epithelial HT29 cell line into mesenchymal cells with a myofibroblast-like phenotype was evaluated. HT29 cultured for 4 days in serum-free Dulbecco's modified Eagle's medium (DMEM) supplemented with 10 ng/mL TGFβ showed a significant increase of ACTA1 and FN1 mRNA levels (183.8% ± 10.6%, $p< 0.001$ and 122% ± 4.6%, $p< 0.001$, respectively) (Fig.6C). The reduced expression of specific intestinal epithelial cell markers, like the GPA33 and KRT20, required a longer exposition time to TGFβ, achieving a significant decrease after 6 days (63.27 % ± 3.8 %,$p< 0,05$ for GPA33 and 49.50 % ± 2.77 %, $p<0,05$ for KRT20) (Fig. 6D). The α-SMA upregulation was confirmed by immunofluorescence assay: 100% of HT29 were α-SMA positive at day 6 of stimulation with 10 ng/mL TGF-β (Fig. 6E)

GED inhibits TGFβ-induced myofibroblast differentiation in a PPARγ-dependent manner

In confluent human intestinal CCD-18Co cell line cultures, the TGF-β-induced upregulation in gene expression of ACTA1 and FN1 was significantly reduced by 1 mM GED (1.66 and 0.8 fold, respectively; $p<0.005$; Fig. 7A). Moreover, GED reduced number of αSMA positive cells after incubation with TGF-β (Fig. 7B).

Furthermore, pre-treatment for 4h with GW, was able to inhibit the ability of GED to reverse the TGFβ-driven upregulation of the evaluated myofibroblasts-like cell markers. These findings suggested that the GED action was directly dependent on PPARγ activation (Fig. 7A and 7B).

GED inhibits epithelial-to-mesenchymal transition

GED was able to regulate EMT by controlling the expression of main markers involved in cell transition. Mesenchymal cells markers, such as ACTA1 and FN1, were overexpressed in monolayers of human intestinal HT29 cell line cultured for 6 days in the presence of 10 ng/ml TGF-β1. In addition, the expression of typical epithelial cells markers, GPA33 and KRT20, was significantly downrgulated under TGF-β stimulation. 1 mM GED administration ameliorated the TGF-β induced 0.9 fold ($p<0.05$) and 2.8 fold ($p< 0.005$) increase of ACTA1 and FN1 expression respectively (Fig. 7C). At the same time, the decreased GPA33 and KRT20 expression, induced by TGF-β, was significantly preserved by the concomitant GED treatment (Fig. 7D). In addition, *de novo* synthesis of αSMA, detected by immunofluorescence assay in 100% of TGF-β-treated cells for 4 days, was reduced by GED (Fig. 7E).

GED reduces the expression of main markers of fibrosis in primary human intestinal fibroblasts

A significant increase of mRNA expression of main markers of fibrosis was observed in primary human intestinal fibroblasts (HIF) obtained from UC patients (HIF-UC) compared to normal control patients (HIF-NC), as shown in Fig. 8. In HIF UC, 24h of GED treatment was able to restore the expression of TGFB1 and ACTA1 to levels comparable to those of

normal fibroblasts, while COL1A1 and FN1 expression was 2.8 and 1.4 fold decreased, compared to not-treated HIF UC (Fig.8).

Discussion

Intestinal fibrosis is a common complication of IBDs; occurring in at least 30-40% of CD and 5% of UC patients. Intestinal fibrosis follows the distribution and location of inflammation[3, 4]. In CD, fibrosis can involve all intestinal layers of the gastrointestinal tract affected by the disease leading to a critical luminal narrowing and obstruction, requiring surgery. In UC, the deposition of ECM is restricted to the mucosal and submucosal layers of the large bowel and can induce structural changes and colonic motility disorders[2-5].

Activated myofibroblasts contribute to ECM deposition. They derive by several sources including resident mesenchymal cells (fibroblasts, sub-epithelial myofibroblasts and smooth muscle cells), stellate cells, pericytes, and intestinal or bone marrow derived stem cells[6, 7]. Recently, epithelial and endothelial cells exposed to pro-fibrotic stimuli have been shown to lose polarity and to acquire a mesenchymal phenotype by two processes known as epithelial-to-mesenchymal transition (EMT) and endothelial-to-mesenchymal transition (EndMT), respectively. During these processes, epithelial and endothelial cells assume a spindle-shape morphology, lose their classical cell markers and gain typical fibroblast or myofibroblast markers and function [29-32].

Over time, it has been widely shown that TGF-β/Smad pathway is mainly accountable for myofibroblasts activation and subsequently fibrosis development.

Briefly, the bind of TGF-β to its specific transmembrane receptor, TGF-β RI, induces phosphorylation of a family of proteins designated as Smads (Smad2 and 3)[7], which form a complex with the common mediator Smad (Co-Smad), Smad4. This complex translocates, thus, in the nucleus and induces expression of target genes. About 60 ECM-related genes were also identified as immediate-early gene targets downstream of TGF-β, such as the myofibroblast activation marker, αSMA, the ECM components, Collagen and Fibronectin, and the downstream mediator, CTGF[7].

Adenovirus-mediated overexpression of TGF-β in the murine colon, for example, leads to colonic fibrosis while conversely the loss of Smad3 confers resistance to 2,4,6-Trinitrobenzenesulfonic acid (TNBS)-induced colorectal fibrosis[16, 17]. All these evidences demonstrate, thus, the pivotal role of TGF-β/Smad pathway in development of intestinal fibrosis, suggesting, hence, that the disruption of TGF-β/Smad pathway could represent the main strategy to improve intestinal fibrosis.

Several researches are, long since, focused on the antagonistic relationship between TGF-β/Smad pathway and PPARγ. Primarily expressed in colorectal mucosa, in vascular tissue and in monocytes, macrophages, dendritic cells, B and T cells, PPARγ is considered like a pivotal actor in the innate antimicrobial immunity and in the control of inflammation [20, 26]. Several natural and synthetic ligands are known to activate PPARγ, such as prostaglandins (PG-D1 and PG-D2) and the PG derivative 15-deoxy-Δ12, 14-PGJ2, thiazolidinediones

(TZD) and 5-ASA. The latter, represents the oldest anti-inflammatory drug used in the treatment of IBD[20, 33, 34].

The PPARγ activation as mediator of the anti-inflammatory action of 5-ASA is already well-established Desreumaux et al.[34]. In addition, genetically engineered PPARγ$^{-/-}$ mice with chemically induced colitis appeared refractory to the anti-inflammatory effect of 5-ASA therapy [27].

Nevertheless, 5-ASA treatments of IBD patients does not prevent nor improves intestinal fibrosis, although the role of PPAR-γ as innate protector against excessive fibrogenesis, is well established[23].

Despite the therapeutic advance in the treatment of IBD in the last two decades, indeed, the incidence of intestinal fibrosis and strictures in CD has not yet significantly changed[5], making a development of efficient anti-fibrotic strategies imperative. The main reasons to assess the efficacy of new synthetic PPARγ modulators in the treatment of intestinal fibrosis are due to the evidences that: (i) together with the adipose tissue, the intestine represents the main site where PPARγ achieves the higher tissue expression levels and (ii) PPARγ activation downregulates TGFβ/Smad pathway[7,13,24,25,35,36].

Evidences for the anti-fibrotic effect of PPARγ are derived from studies focused on liver fibrosis, where PPARγ activation reverted the activated phenotype of hepatic stellate cells (HSCs) [37]. The ability of PPARγ to improve hepatic fibrosis was established by using TZDs, a class of insulin-sensitizing PPARγ agonists widely used in the treatment of type 2 diabetes. TZDs reduce ECM production, HSC proliferation and migration, suppress pro-inflammatory and pro-fibrotic cytokines and chemokines and induce apoptosis in HSC[37-42].

In the present study, we assess the effects of the PPARγ modulator GED in the DSS-induced chronic colitis and fibrosis in mice. We demonstrate that the macroscopic and microscopic inflammatory lesions associated with chronic DSS administration, as well as the collagen deposition in the *mucosa*, *submucosa* and *serosa layers* were improved by daily oral GED administration and not by 5ASA.

In addition, the gene overexpression of α-SMA, Collagen and Fibronectin and the increase of their tissue protein levels is specifically improved by GED, while 5-ASA does not induce any significant regulation of their expression.

The main TGFβ/Smad pathway components and related pro-fibrotic molecules like IL-13 and CTGF, are also observed.

The relevance of IL-13 in fibrotic process has been demonstrated in various organs including the intestine[43-46]. In TNBS-induced colitis, fibrosis development depends upon IL-13 binding to the IL-13 receptor to induce TGF-β. In the same way, if IL-13 signaling is inhibited TGF-β is produced in reduced amounts and fibrosis does not occur[45, 46]. On the other side, CTGF has been shown to be co-expressed with TGFβ in multiple fibrotic disorders, including intestinal fibrosis, and is considered a key driver of fibrosis[7, 13]. CTGF

is, indeed, the main downstream effector of TGF-β/Smad3 pathway that induces cell proliferation, ECM proteins and tissue inhibitor of metalloproteinase (TIMPs) expression and inhibits matrix metalloproteinase (MMPs)[7, 47-50]. In addition, CTGF inhibition might block the pro-fibrotic effects of TGF-β, without affecting its immunoregulatory effects[47, 48]. Various compounds targeting CTGF have shown strong anti-fibrotic properties [48].

We find that daily GED treatments in mice with DSS-induced chronic colitis dowregulated expression of TGF-β, Smad 3, IL-13 and CTGF, effects not observed with 5-ASA administration.

In addition, we demonstrate that the specific antifibrotic properties of GED is dependent by the specific activation of PPARγ. Indeed, the combined association of GED administration with GW9662, a specific irreversible antagonist of PPARγ, completely abrogates the ability of GED to control the main events associated with intestinal fibrosis, in a murine model of DSS-induced chronic colitis.

Moreover, since the main progenitor cells of activated myofibroblasts are the fibroblasts and the epithelial cells, the latter through the process of EMT, we have evaluated *in vitro* the GED action on the TGFβ-induced differentiation both of human intestinal fibroblast (CCD-18Co) and epithelial (HT29) cell lines into activated ECM-producing myofibroblasts, as well as in primary human intestinal fibroblasts.

Fibroblasts are a heterogeneous population of cells present in the interstitium of all normal tissues and organs where they play a pivotal role in maintaining structural integrity by regulating matrix homeostasis and they are directly involved in healing and regenerative processes, as well as fibrosis. During chronic tissue injury, fibroblasts acquire a myofibroblastic phenotype and produce large amounts of ECM proteins with different architectural and barrier functions and regulate several growth factors acting in a paracrine and autocrine fashion[2, 7, 29, 51]. The increased expression of both αSMA and fibronectin, induced by TGF-β stimulation, were reduced by GED in our intestinal fibroblast cell line and this effect was completely abrogated by a pre-treatment with GW, a specific antagonist of PPARγ, demonstrating that the PPARγ activation represents the pivotal event of the GED action.

In addition, the anti-fibrotic GED properties were also assessed on primary human intestinal fibroblasts obtained from colonic surgical specimens of UC patients and compared with fibroblasts isolated from healthy colonic surgical specimens. GED significantly reduced the higher expression of α-SMA, fibronectin, Collagen I-III and TGF-β observed in colonic fibroblast from UC.

Finally, the effects of GED on TGF-β induced EMT were assessed. GED administration was able to block the TGF-β-dependent transition process of the intestinal epithelial HT29 cell line into ECM-producing mesenchymal cells, controlling αSMA and fibronectin expression and reverting the TGF-β-induced GPA33 and KRT20 downregulation, two of the main intestinal epithelial cells markers.

In conclusion, the new 5-ASA analogue GED-0507-34 Levo, has shown consistent anti-fibrotic properties both *in vivo* and *in vitro*, specifically mediated by PPARγ. GED-0507-34 Levo was able to reduce the activation state of myofibroblasts and the expression of the main pro-fibrotic molecules including TGF-β, Smad3, IL13, and CTGF.

The conventional view of considering intestinal fibrosis in IBD as an inevitable and irreversible process is progressively changing in light of the improved knowledge of the cellular and molecular mechanisms leading to fibrosis. Comprehension of the mechanisms of intestinal fibrosis may pave the way for the developments of efficacious and specific anti-fibrotic agents. Sspecific PPARγ ligands like the GED-0507-34 Levo, with both anti-inflammatory and anti-fibrotic properties, could be a new possible therapeutic approach for IBD.

Acknowledgments

This study was supported by the University of L'Aquila, L'Aquila, Italy; the Nogra Pharma Ldt.; the Intestinal Biotech Development of Lille, France; the Digest Science foundation and the association F. Aupetit, Lille, France. We thank also the Prof. Fiocchi of the Department of Pathobiology, Cleveland Clinic Foundation, Cleveland, Ohio, USA for suggestions and discussion.

Sources of support that require acknowledgment: This study was supported by the University of L'Aquila, L'Aquila, Italy; the Inserm U995, Lille, France; the Nogra Pharma Ldt; the Intestinal Biotech Development of Lille, France; the Digest Science foundation and the association F. Aupetit, Lille, France.

Source of Funding: Speca Silvia, Rousseaux Christel, Dubuquoy Caroline, have financial disclosure in the field of PPARγ research with Nogra Pharma Ldt. Pierre Desreumaux has the following conflicts of interest for consulting fees, lecture fees or grant supports with Nogra Pharma Ldt, Procter and Gamble, London, UK, Shire Pharmaceuticals, USA and Lesaffre, Marcq en Baroeul, France. Giovanni Latella has consulted to MSD Italy and Shire; has received research grants from Nogra Pharma Ldt, Alfa Wassermann Italy and Sofar Italy.

References

1. Wynn TA, Ramalingam TR. Mechanisms of fibrosis: therapeutic translation for fibrotic disease. Nat Med. 2012; 18:1028–1040. [PubMed: 22772564]
2. Fiocchi C, Lund PK. Themes in fibrosis and gastrointestinal inflammation. Am J Physiol Gastrointest Liver Physiol. 2011; 300:677–683.
3. Rieder F, Fiocchi C. Intestinal fibrosis in IBD-a dynamic, multifactorial process. Nat Rev Gastroenterol Hepatol. 2009; 6:228–235. [PubMed: 19347014]
4. Burke JP, Mulsow JJ, O'Keane C, et al. Fibrogenesis in Crohn's disease. Am J Gastroenterol. 2007; 102:439–448. [PubMed: 17156147]
5. Rieder F, Zimmermann EM, Remzi FH, et al. Crohn's disease complicated by strictures: a systematic review. Gut. 2013; 62:1072–1084. [PubMed: 23626373]
6. Rieder F, Karrasch T, Ben-Horin S, et al. Results of the 2nd scientific workshop of the ECCO (III): basic mechanisms of intestinal healing. J Crohns Colitis. 2012; 6:373–385. [PubMed: 22405177]
7. Speca S, Giusti I, Rieder F, et al. Cellular and molecular mechanisms of intestinal fibrosis. World J Gastroenterol. 2012; 18:3635–3661. [PubMed: 22851857]
8. Verrecchia F, Mauviel A. Transforming Growth Factor-beta Signaling Through the Smad Pathway: Role in Extracellular Matrix Gene Expression and Regulation. J Invest Dermatol. 2002; 118:211–215. [PubMed: 11841535]
9. Verrecchia F, Chu ML, Mauviel A. Identification of novel TGF-beta/Smad gene targets in dermal fibroblasts using a combined cDNA microarray/promoter transactivation approach. J Biol Chem. 2001; 276:17058–17062. [PubMed: 11279127]
10. Inagaki Y, Okazaki I. Emerging insights into transforming growth factor α/smad signal in hepatic fibrogenesis. Gut. 2007; 56:284–292. [PubMed: 17303605]

11. Bonniaud P, Margetts PJ, Ask K, et al. TGF-β and Smad3 signaling link inflammation to chronic fibrogenesis. J Immunol. 2005; 175:5390–5395. [PubMed: 16210645]
12. Gauldie J, Bonniaud P, Sime P, et al. TGF-beta, Smad3 and the process of progressive fibrosis. Biochem Soc Trans. 2007; 35:661–664. [PubMed: 17635115]
13. Latella G, Rogler G, Bamias G, et al. Results of the 4th scientific workshop of the ECCO (I): Pathophysiology of intestinal fibrosis in IBD. J Crohns Colitis. 2014; 8:1147–1165. [PubMed: 24731838]
14. Di Sabatino A, Jackson CL, Pickard KM, et al. Transforming growth factor beta signalling and matrix metalloproteinases in the mucosa overlying Crohn's disease strictures. Gut. 2009; 58:777–789. [PubMed: 19201776]
15. Rieder F, Kessler S, Sans M, et al. Animal models of intestinal fibrosis: new tools for the understanding of pathogenesis and therapy of human disease. Am J Physiol Gastrointest Liver Physiol. 2012; 303:G786–801. [PubMed: 22878121]
16. Vallance BA, Gunawan MI, Hewlett B, et al. TGF-beta1 gene transfer to the mouse colon leads to intestinal fibrosis. Am J Physiol Gastrointest Liver Physiol. 2005; 289:G116–28. [PubMed: 15778431]
17. Latella G, Vetuschi A, Sferra R, et al. Smad3 loss confers resistance to the development of trinitrobenzene sulfonic acid-induced colorectal fibrosis. Eur J Clin Invest. 2009; 39:145–156. [PubMed: 19200168]
18. Wei J, Ghosh AK, Sargent JL, et al. PPARγ downregulation by TGFβ in fibroblast and impaired expression and function in systemic sclerosis: a novel mechanism for progressive fibrogenesis. PLoS One. 2010; 5:e13778. [PubMed: 21072170]
19. Ghosh AK, Bhattacharyya S, Wei J, et al. Peroxisome proliferator-activated receptor-gamma abrogates Smad-dependent collagen stimulation by targeting the p300 transcriptional coactivator. FASEB J. 2009; 23:2968–2977. [PubMed: 19395477]
20. Dubuquoy L, Rousseaux C, Thuru X, et al. PPARgamma as a new therapeutic target in inflammatory bowel diseases. Gut. 2006; 55:1341–1349. [PubMed: 16905700]
21. Yang L, Stimpson SA, Chen L, et al. Effectiveness of the PPARγ agonist, GW570, in liver fibrosis. Inflamm Res. 2010; 59:1061–1071. [PubMed: 20585829]
22. Rieder F, Georgieva M, Schirbel A, et al. Prostaglandin E2 inhibits migration of colonic lamina propria fibroblasts. Inflamm Bowel Dis. 2010; 16:1505–1513. [PubMed: 20803697]
23. Latella G, Sferra R, Speca S, et al. Can we prevent, reduce or reverse intestinal fibrosis in IBD? Eur Rev Med Pharmacol Sci. 2013; 17:1283–1304. [PubMed: 23740440]
24. Kawai T, Masaki T, Doi S, et al. PPAR-gamma agonist attenuates renal interstitial fibrosis and inflammation through reduction of TGF-beta. Lab Invest. 2009; 89:47–58. [PubMed: 19002105]
25. Aoki Y, Maeno T, Aoyagi K, et al. Pioglitazone, a peroxisome proliferator-activated receptor gamma ligand, suppresses bleomycin-induced acute lung injury and fibrosis. Respiration. 2009; 77:311–319. [PubMed: 18974632]
26. Speca S, Dubuquoy L, Desreumaux P. Peroxisome Proliferator-activated Receptor Gamma in the Colon: Inflammation and Innate Antimicrobial Immunity. J Clin Gastroenterol. 2014; 48:23–27.
27. Bertin B, Dubuquoy L, Colombel JF, et al. PPAR-gamma in ulcerative colitis: a novel target for intervention. Curr Drug Targets. 2013; 14:1501–1507. [PubMed: 23651165]
28. Livak KJ, Schmittgen TD. Analysis of relative gene expression data using real-time quantitative PCR and the 2(-Delta Delta C(T)) Method. Methods. 2001; 25:402–8. [PubMed: 11846609]
29. Pucilowska JB, Williams KL, Lund PK. Fibrogenesis IV. Fibrosis and inflammatory bowel disease: cellular mediators and animal models. Am J Physiol Gastroinest Liver Physiol. 2000; 279:G653–659.
30. Lee J, Dedhar S, Kalluri R, et al. The epithelial-mesenchymal transition: new insights in signaling, development, and disease. J Cell Biol. 2006; 172:973–981. [PubMed: 16567498]
31. Flier SN, Tanjore H, Kokkotou EG, et al. Identification of epithelial to mesenchymal transition as a novel source of fibroblasts in intestinal fibrosis. J Biol Chem. 2010; 285:20202–20212. [PubMed: 20363741]

32. Rieder F, Kessler SP, West GA, et al. Inflammation-induced endothelial-to-mesenchymal transition: a novel mechanism of intestinal fibrosis. Am J Pathol. 2011; 179:2660–2673. [PubMed: 21945322]
33. Pirat C, Farce A, Lebègue N, et al. Targeting peroxisome proliferator-activated receptors (PPARs): development of modulators. J Med Chem. 2012; 55:4027–4061. [PubMed: 22260081]
34. Desreumaux P. Understanding the Mechanism of 5-ASA in Treating Colonic Inflammation. Gastroenterol Hepatol. 2008; 4:319–320.
35. Zhao C, Chen W, Yang L, et al. PPARgamma agonists prevent TGFbeta1/Smad3-signaling in human hepatic stellate cells. Biochem Biophys Res Commun. 2006; 350:385–391. [PubMed: 17010940]
36. Zhang GY, Cheng T, Zheng MH, et al. Activation of peroxisome proliferator-activated receptor-gamma inhibits transforming growth factor-beta1 induction of connective tissue growth factor and extracellular matrix in hypertrophic scar fibroblasts in vitro. Arch Dermatol Res. 2009; 301:515–522. [PubMed: 19466435]
37. Galli A, Crabb D, Price D, et al. Peroxisome proliferator-activated receptor gamma transcriptional regulation is involved in platelet-derived growth factor-induced proliferation of human hepatic stellate cells. Hepatology. 2000; 31:101–108. [PubMed: 10613734]
38. Xu HE, Lambert MH, Montana VG, et al. Structural determinants of ligand binding selectivity between the peroxisome proliferator-activated receptors. Proc Atl Acad Sci USA. 2001; 98:13919–13924.
39. Galli A, Crabb DW, Ceni E, et al. Antidiabetic thiazolidinediones inhibit collagen synthesis and hepatic stellate cell activation in vivo and in vitro. Gastroenterology. 2002; 122:1924–1940. [PubMed: 12055599]
40. Marra F, Efsen E, Romanelli RG, et al. Ligands of peroxisome proliferator-activated receptor gamma modulate profibrogenic and proinflammatory actions in hepatic stellate cells. Gastroenterology. 2000; 119:466–478. [PubMed: 10930382]
41. Miyahara T, Schrum L, Rippe R, et al. Peroxisome proliferator-activated receptors and hepatic stellate cell activation. J Biol Chem. 2000; 275:35715–35722. [PubMed: 10969082]
42. Planaguma A, Claria J, Miquel R, et al. The selective cyclooxygenase-2 inhibitor SC-236 reduces liver fibrosis by mechanisms involving non-parenchymal cell apoptosis and PPARgamma activation. FASEB J. 2005; 19:1120–1122. [PubMed: 15876570]
43. Chiaramonte MG, Donaldson DD, Cheever AW, et al. An IL-13 inhibitor blocks the development of hepatic fibrosis during a T-helper type 2-dominated inflammatory response. J Clin Invest. 1999; 104:777–785. [PubMed: 10491413]
44. Chiaramonte MG, Cheever AW, Malley JD, et al. Studies of murine schistosomiasis reveal interleukin-13 blockade as a treatment for established and progressive liver fibrosis. Hepatology. 2001; 34:273–282. [PubMed: 11481612]
45. Fichtner-Feigl S, Strober W, Kawakami K, et al. IL-13 signaling through the IL-13alpha2 receptor is involved in induction of TGF-beta1 production and fibrosis. Nat Med. 2006; 12:99–106. [PubMed: 16327802]
46. Fichtner-Fiegl S, Strober W, Geissler EK, et al. Cytokines mediating the induction of chronic colitis and colitis-associated fibrosis. Mucosal Immunol. 2008; 1:S24–S27. [PubMed: 19079223]
47. Dammeier J, Brauchle M, Falk W, et al. Connective tissue growth factor: a novel regulator of mucosal repair and fibrosis in inflammatory bowel disease? Int J Biochem Cell Biol. 1998; 30:909–922. [PubMed: 9744082]
48. di Mola FF, Di Sebastiano P, Gardini A, et al. Differential expression of connective tissue growth factor in inflammatory bowel disease. Digestion. 2004; 69:245–253. [PubMed: 15256831]
49. Somerville RP, Oblander SA, Apte SS. Matrix metalloproteinases: old dogs with new tricks. Genome Biol. 2003; 4:216. [PubMed: 12801404]
50. Kossakowska AE, Edwards DR, Lee SS, et al. Altered balance between matrix metalloproteinases and their inhibitors in experimental biliary fibrosis. Am J Pathol. 1998; 153:1895–1902. [PubMed: 9846979]
51. Rieder F, Fiocchi C. Intestinal fibrosis in inflammatory bowel disease: progress in basic and clinical science. Curr Opin Gastroenterol. 2008; 24:462–468. [PubMed: 18622160]

List of Abbreviations

5-ASA	5-Aminosalicylic Acid
Acta1/ACTA2	mouse/human gene encoding αSMA
CD	Crohn's Disease
KRT20	human gene encoding Cytokeratin 20
CTGF	Connective tissue growth factor
DSS	Dextran sulfate sodium
ECM	Extracellular matrix
EMT	Epithelial-to-mesenchymal transition
EndMT	Endothelial-to-mesenchymal transition
Fn1/FN1	mouse/human gene encoding Fibronectin
GAPDH	glyceraldehyde-3-phosphate dehydrogenase
GPA33	human gene encoding glycoprotein A33
HIF	Human intestinal fibroblasts
IBD	Inflammatory Bowel Disease
IEC	Intestinal epithelial cells
IL	interleukin
NF-κB	Nuclear Factor-κB
PPARγ	Peroxisome-proliferator activated receptor
Smad	small mother against decapentaplegic
TGF-β	Transforming growth factor β
TNBS	2,4,6-Trinitrobenzenesulfonic acid
TZD	Thiazolidinediones
UC	Ulcerative Colitis
αSMA	alpha Smooth Muscle Actin

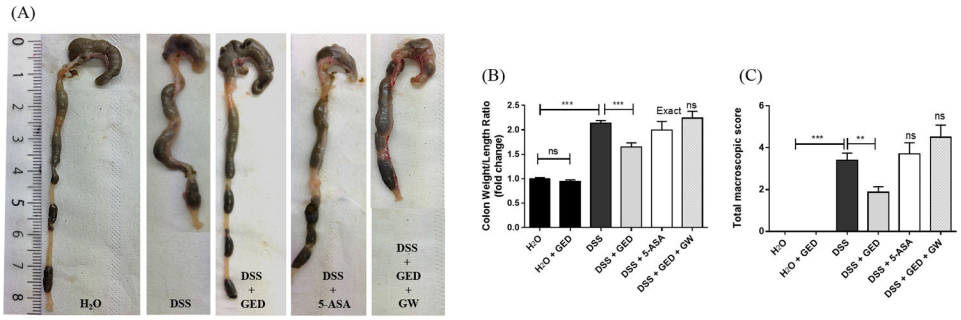

Fig. 1.

(A) Macroscopic appearance of the colons from the mice in five different groups: i. control group (CTRL group); ii. DSS-treated mice (DSS group); iii. DSS-treated mice receiving 30 mg/kg/day GED (DSS+GED group); iv. DSS-treated mice receiving 150 mg/kg/day 5-ASA (DSS + 5-ASA group); v. DSS-treated mice receiving both 30 mg/kg/day GED and 1 mg/Kg/day GW9662 (DSS + GED + GW group). The colon from DSS mice appeared shorter and dilated and displayed thickened walls compared to the colon both from CTRL and DSS + GED mice. The colon from DSS + 5-ASA group appeared longer but still dilated compared to DSS group, while any amelioration was observed in colon from DSS + GED + GW9662 group compared to DSS group. **(B)** DSS-treated mice showed a significant increase of the colon weight/length ratio compared to CTRL group and DSS + GED group. Not significant differences in the weight/length ratio of colon were observed in mice receiving 5-ASA and GED + GW9662 compared to DSS group. **(C)** Total macroscopic score calculated as sum of the score of individual macroscopic colonic lesions (adhesions, thickness and dilation) on a 0–2 scale, for each group. Colon from DSS group showed a significant increase of the total macroscopic score compared to CTRL group and DSS + GED. Any significant amelioration was observed in DSS-treated mice receiving both 5-ASA and GED + GW9662. Data are expressed as mean ± SEM of two independent experiments; **= $p< 0.01$ and ***= $p<0,005$. ns= not significant

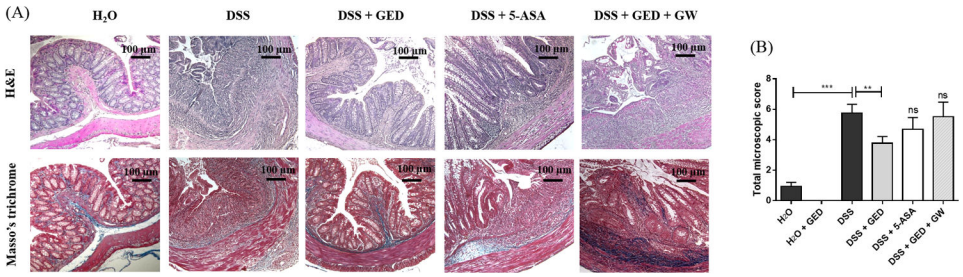

Fig. 2.

(A) Degree of colonic inflammation and of fibrosis was assessed by Haematoxilin and Eosin and Masson's trichrome stainings, respectively. Representative histologic sections of distal colon are shown. DSS mice showed signs of severe chronic inflammation and marked fibrosis. Daily GED administration restablished normal mucosa architecture with a very low fibrotic degree in the submucosa. DSS-treated mice receiving 5-ASA still showed an high degree of damage in *lamina propria* and submucosa while GED effect in DSS-treated mice was lost when combined with GW9662. **(B)** The total microscopic score is significantly higher in DSS mice and is significantly reduced by GED administration. Not significant improvement of the total microscopic score was induced by 5-ASA administration and by GED treatment when combined with GW9662. Data are expressed as mean ± SEM of two independent experiments; **= p< 0.01 and ***= p<0,005.

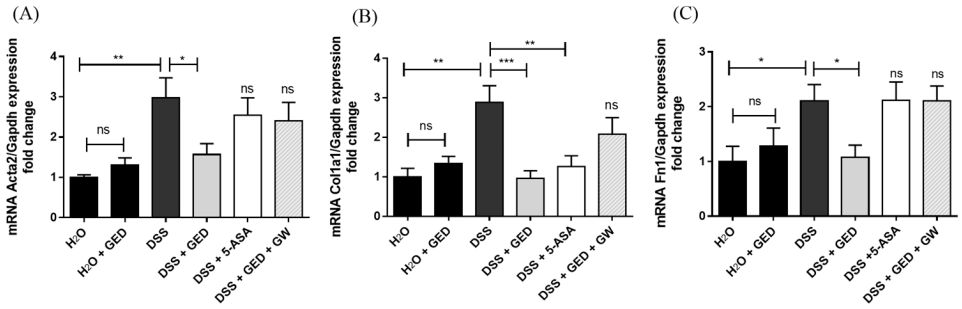

Fig. 3.

Relative expression of the profibrotic genes, Acta2, COL1a1 and Fn1 was determined by quantitative RT-PCR. The significant increase of mRNA expression of Acta2, COL1a1 and Fn1, observed in DSS group, was regulated by GED. 5-ASA administration significantly regulated COL1a1 but not Acta2 and Fn1 gene expression. The GED effect in DSS-treated mice was lost in combination with GW9662. Data are presented as mean of fold change vs CTRL. *= $p<0.05$, ***= $p<0.005$. ns= not significant

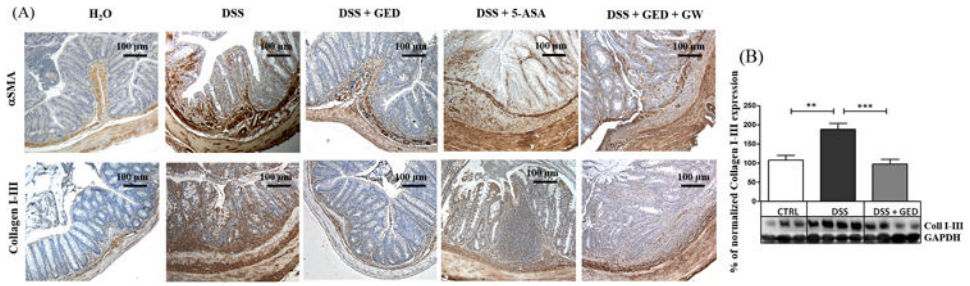

Fig. 4.

(A). Representative immunohistological staining microphotographs of distal colonic sections and the related quantitative analysis on the digital image showing an increased α-SMA (in *submucosa*, *muscolaris propria* and serosal layer) and Collagen I-III (in all colon wall layers) expression in the DSS mice. GED treatment leaded to a reduction of both fibrotic markers. DSS-treated mice receiving 5-ASA did not show decreased expression of α-SMA and Collagen I-III, while GED effect in DSS-treated mice was lost when combined with GW9662. **(B)** A significant reduction of Collagen expression induced by GED is also confirmed by immunoblotting assay. Representative immunoblots are shown and bar graphs represent the % of mean ± SEM of normalized Collagen quantity, determined by densitometric analysis. **= $p<0.01$ and ***= $p<0.005$.

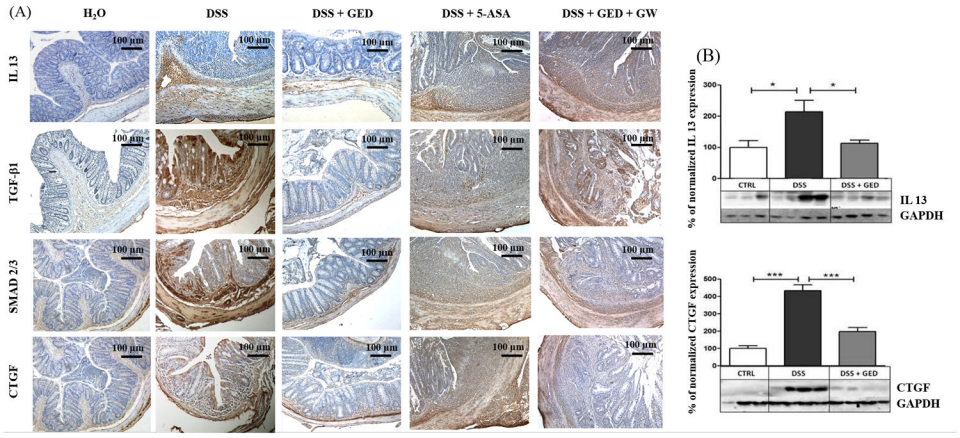

Fig. 5.

(A) The immunohistochemistry microphotographs on digital image showed a significant upregulation of all four examined markers (IL-13, TGFβ, Smad3, CTGF) in *submucosa*, *muscolaris propria* and serosal layers of DSS-treated mice. GED administration induced a complete restoration in the expression of all markers. GED effect in DSS-treated mice was lost when combined with GW9662. DSS-treated mice receiving 5-ASA did not show decreased expression of the observed markers. **(B)** A significant downregulation of IL-13 and CTGF induced by GED administration is confirmed by immunoblotting assay. Representative blots are shown and data are presented as mean of fold change vs CTRL. *= $p< 0.05$, ***= $p<0.005$.

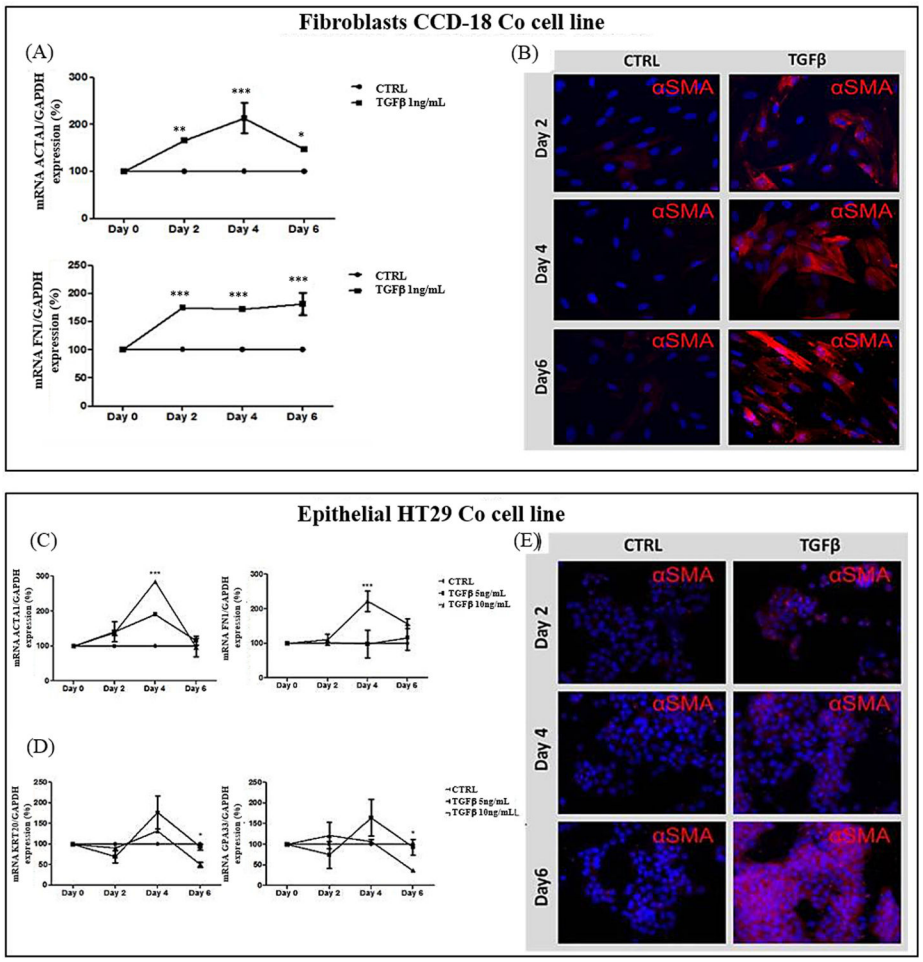

Fig. 6.

(A) An increased expression of ACTA1 and FN1 genes was induced in monolayers of human CCD-18Co exposed to TGF-β1 1 ng/ml for 2, 4 and 6 day in serum-free Eagle's MEM. **(B)** The increased expression of α-SMA in TGFβ-stimulated CCD-18Co cultures was also confirmed by immunofluorescence staining (red) on day 2, 4 and 6 and accompanying phase images of cell morphology were obtained. **(C)** Confluent human HT29 was incubated with TGF-β 5 and 10 ng/ml for 2, 4 and 6 day in serum-free Eagle's MEM. TGF-β 10 ng/ml led, at day 4, to a significant increase of both mRNA ACTA1 and FN1 expression levels. **(D)** TGF-β 10 ng/ml reduced, at day 6, the mRNA expression of intestinal epithelial cell markers, like KRT20 and GPA33. **(E)** At day 6, a marked increase of αSMA expression in TGFβ-stimulated HT-29 cultures was also confirmed by immunofluorescence staining (red). *= $p<0.05$, **= $p<0.01$ and ***= $p<0.005$.

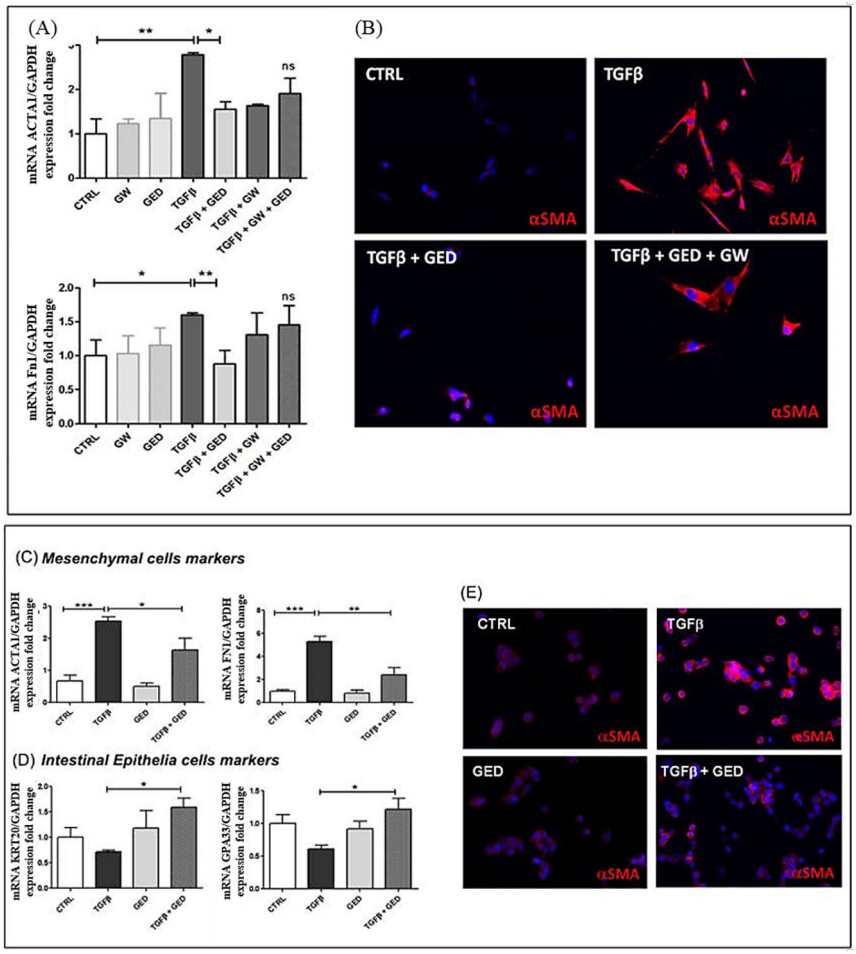

Fig. 7.

(A) Monolayers of CCD-18Co cultures showed increased mRNA expression of ACTA1 and FN1, induced by 4 days of TGF-β stimulation. GED 1mM reduced upregulation of these markers and this effect is completely abrogated by a pre-treatment with GW. **(B)** The marked immunoreactivity for α-SMA (red) in TGFβ-stimulated CCD-18Co cultures, at day 4, is completely abrogated by GED and reversed by the pre-treatment with GW. Phase images of cell morphology were obtained. **(C)** In monolayers of human intestinal HT29 cell line cultures, the TGF-β-induced expression of ACTA1 and FN1 was significantly reduced by the concomitant addition of GED into cultures. **(D)** In HT29 cell line cultures, GED prevented the TGF-β-induced downregulation of GPA33 and KRT20, two epithelial cells markers. **(E)** The increased α-SMA expression in TGFβ-stimulated HT-29 cultures was strongly reduced by the concomitant treatment with GED. *= $p<0.05$, **= $p<0.01$ and ***= $p<0.005$, ns= not significant.

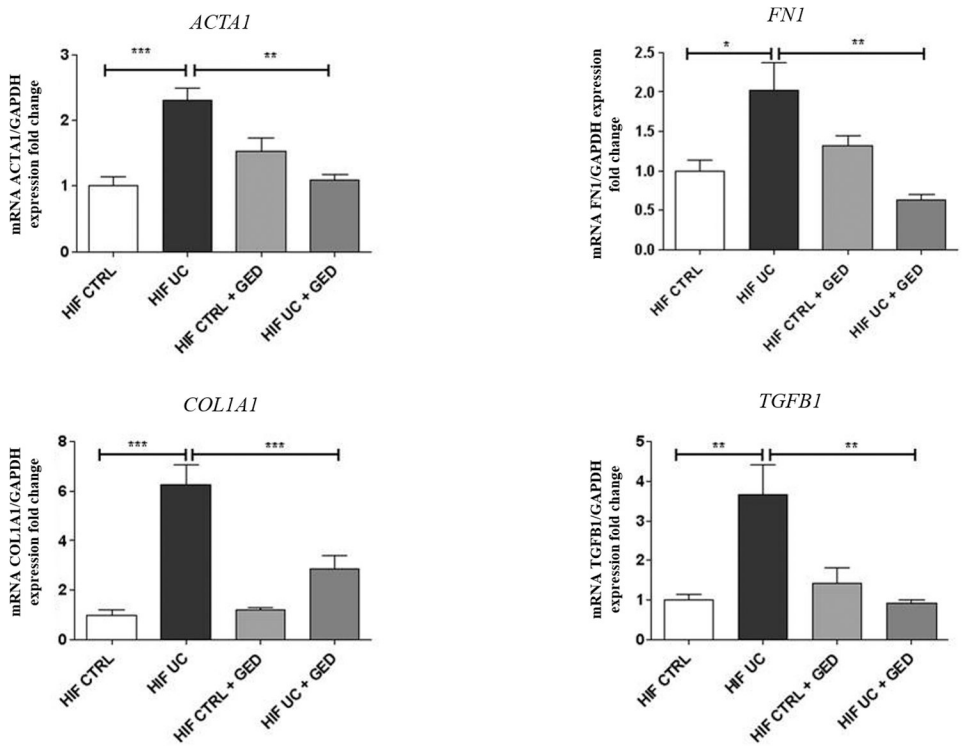

Fig. 8.

The high mRNA levels of ACTA1, COL1A1, FN1 and TGFB observed in HIF-UC were significantly reduced by GED.

Table 1

1 Primer sequences for quantitative RT-PCR

Gene	Source	NCBI Reference Sequence	Primer	Sequences (5′ →3′)
Acta2	Mouse	NM_007392.3	Forward	CCT GAC GGG CAG GTG ATC
			Reverse	ATG AAA GAT GGC TGG AAG AGA GTC T
COL1a1	Mouse	NM_007742.3	Forward	GAG TAC TGG ATC GAC CCT AAC CAA
			Reverse	ACA CAG GTC TGA CCT GTC TCC AT
Fn1	Mouse	NM_001276408.1	Forward	CGAAGCCGGGAAGAGCAAG
			Reverse	CGTTCCCACTGCTGATTTATCTG
GAPDH	Mouse	NM_001289726.1	Forward	ATG GGA AGC TTG TCA TCA ACG
			Reverse	GGC AGT GAT GGC ATG GAC TG
ACTA1	Human	NM_001100.3	Forward	CCTTCCAGCAGATGTGGATCA
			Reverse	AAGCATTTGCGGTGGACAA
FN1	Human	NM_001306129.1	Forward	GATGCTCCCACTAACCTCCA
			Reverse	CGGTCAGTCGGTATCCTGTT
KRT20	Human	NM_019010.2	Forward	TCCCAGAGCCTTGAGATAGAACTC
			Reverse	GTTGGCTAACTGGCTGTAAC
GPA33	Human	NM_005814	Forward	AGAAGCAAGACCATGGTGGG
			Reverse	GTGACACTCTTTCCCTGCGA
COL1A1	Human	NM_000088.3	Forward	TGGGCGGGAGAGACTGTTC
			Reverse	TGCCCCGGTGACACATC
TGFB1	Human	NM_000660.5	Forward	AACCCACAACGAAATCTATGACAAG
			Reverse	AGAGCAACACGGGTTCAGGTA
GAPDH	Human	NM_001256799.2	Forward	GACACCCACTCCTCCACCTTT
			Reverse	TTGCTGTAGCCAAATTCGTTGT

Table 2

Effect of GED Administration on Course and Macroscopic Findings of DSS-induced chronic colitis

Parameters	H_2O	H_2O + GED	DSS	DSS + GED	DSS + 5-ASA	DSS + GED + GW
Duration of DSS treatment (days)	36	36	24	24	24	24
Number of mice	20	10	35	35	10	10
Mortality (n. mice)	0	0	2	0	0	0
Colon weight (g)	0,171 ± 0,004	0,154 ± 0,007	0,29 ± 0,007***	0,25 ± 0,01¥	0,25 ± 0,02*ns*	0,25 ± 0,014*ns*
Colon length (cm)	8,79 ± 0,14	9,24 ± 0,36	6,89 ± 0,11***	7,29 ± 0,011¥¥	7,22 ± 0,25 *ns*	6,42 ± 0,2615 *ns*
Colon weight/length ratio (g/cm)	1,003 ± 0,02	0,94 ± 0,04	2,14 ± 0,05***	1,65 ± 0,09¥¥¥	2,00 ± 0,17 *ns*	2,24 ± 0,1407 *ns*
Dilation	np	np	1,55 ± 0,13**	1,02 ± 0,14¥	0,9 ± 0,27*ns*	1,3 ± 0,26*ns*
Thickness	np	np	1,18 ± 0,13***	0,58 ± 0,11¥¥	1,6 ± 0,22*ns*	1,7 ± 0,2134*ns*
Adhesions	np	np	0,88 ± 0,19**	0,41± 0,11*ns*	1,2 ± 0,25*ns*	1,5 ± 0,268*ns*
Total macroscopic score	np	np	3,6 ± 0,34***	2,02 ± 0,27¥¥	3,7 ± 0,54*ns*	4,5 ± 0,5821*ns*

Data are expressed as mean ± SEM; np= not present;

* = p< 0.05 vs H_2O;

** = p< 0.01 vs H_2O;

*** = p< 0,005 vs H_2O;

¥ = p< 0.05 vs DSS;

¥¥ = p< 0,01 vs DSS;

¥¥¥ = p< 0,005 vs DSS.

ns = not significant